ELSEVIER

Journal of Photochemistry and Photobiology A: Chemistry 123 (1999) 109–119

Journal of Photochemistry and Photobiology A:Chemistry

Dual fluorescence of 2-(4′-*N*,*N*-dimethylaminophenyl)benzimidazole: effect of β-cyclodextrin and pH

G. Krishnamoorthy, Shen K. Dogra*

Department of Chemistry, Indian Institute of Technology, Kanpur 208016, India

Received 5 November 1998; received in revised form 20 January 1999; accepted 22 January 1999

Abstract

Spectral characteristics of 2-(4′-*N*,*N*-dimethylaminophenyl)benzimidazole (DMAPBI) and its monocations have been studied in aqueous β-cyclodextrin (β-CDx) solutions. Blue shifts observed in the twisted intramolecular charge transfer (TICT) band (A band) and enhancement in its emission intensity are larger than those observed in the locally excited (B band) state. Two kinds of monocations (MC) are present in aqueous medium: the MC1 protonated at $-NMe_2$ group and the MC2 protonated at =N– atom. The former is present in a very small amount in comparison to the latter and is also supported by the fluorescence excitation spectra. Similar lifetimes observed for both the bands of neutral DMAPBI in aqueous and β-CDx media suggest that equilibrium is established between the A and B states. Further, only one kind of inclusion complex (1 : 1) is established between β-CDx and neutral DMAPBI. Fluorescence spectra, fluorescence excitation spectra, different values of binding constants observed at 440 and 520 nm, and time correlated studies suggest that the MC2 forms two kinds of inclusion complexes with β-CDx. Spectral characteristics of the neutral and the MC of DMAPBI suggest that $-NMe_2$ group is buried in the non-polar cavity of β-CDx.

Keywords: Fluorescence; *N*,*N*-dimethylaminophenyl(benzimidazole); β-Cyclodextrin

1. Introduction

Cyclodextrins (CDx) are water soluble molecules containing hydrophobic cavity. The size of hydrophobic cavity depends on the number of gluocopyranose units present in the CDx. For example α-, β- and γ-CDx are oligosaccharides containing six, seven and eight units of gluocopyranose units, respectively [1,2]. Thus CDx are capable of incorporating a wide range of guest molecules depending upon their size, shape and hydrophobic character [3–5]. Further, depending upon the size of the guest molecules, different component ratios of substrates to CDx complexes are observed that can change the photophysical and chemical properties of the hydrophobic organic molecules in aqueous solutions, e.g. solubility [6], enhancement in the absorbance and the fluorescence intensity [7,8], acid–base characteristics [9], excited state intramolecular proton transfer [10–12] etc. All this information can throw light on the structures of molecules in solutions.

Recently, photophysical properties of the molecule showing TICT behaviour have been studied in CDx/water environments [13–17]. The reasons being that the emission properties of both the bands, especially those of the TICT band, are very sensitive to the environments [18–22]. It has been noticed that these changes observed in the TICT (A band) and the normal (B band) fluorescence bands depend upon the size of CDx as well as on the size of the substrate. In other words, the molecules showing TICT behaviour can be present in different parts of the CDx. In the present work, we report our work on the fluorescence characteristics of 2-(4′-*N*,*N*-dimethylaminophenyl)benzimidazole (DMAPBI) dissolved in aqueous solutions of β-CDx. The reason being that the DMAPBI molecule is quite big and can be encapsulated only lengthwise. Acid–base equilibrium has also been studied to find the location of the molecule in β-CDx.

2. Methods and materials

DMAPBI was obtained by heating *o*-phenylenediamine with *p*-(dimethylamino)benzoic acid in polyphosphoric acid, using the procedure described for 2-substituted benzimidazoles [23]. The product was purified by repeated recrystallization from aqueous ethanol. The purity of the compound was checked by TLC and by verifying that the

*Corresponding author. Tel: +91-512-597163; fax: +91-512-597438/590007/590260; e-mail: skdogra@iitk.ernet.in

1010-6030/99/$ – see front matter
PII: S1010-6030(99)00030-1

fluorescence excitation spectrum in methanol was identical when the emission was monitored at different wavelengths. β-CDx was obtained from Aldrich chemical company and used as received. Triply distilled water was used for preparing aqueous solutions. A stock solution of DMAPBI was prepared in methanol. The final concentration of DMAPBI for recording the spectra, evaluating fluorescence quantum yields (ϕ_{fl}) and determining the excited state lifetime was 2×10^{-5} M, containing less than 0.5% (v/v) methanol. The pH of the solutions in the range of 2–9 were adjusted by adding small amounts of NaOH or H_2SO_4. The instruments used to record absorption and fluorescence spectra to determine the lifetimes, and the procedure used to determine ϕ_{fl} have been described elsewhere [24,25].

3. Results and discussion

3.1. Spectral characteristics of DMAPBI under neutral conditions

The absorption spectra of DMAPBI recorded at different β-CDx concentrations and at pH 8 are shown in Fig. 1. The long wavelength (LW) absorption band maximum is slowly red shifted from 328 to 333 nm, with a gradual increase in the molecular extinction coefficient. This increase in the absorbance is due to the encapsulation of DMAPBI into β-CDx and is attributed to the detergent action of β-CDx as observed by others also [10,26]. No clear isosbestic point is observed in the absorption spectra, but the changes that are observed in the absorbance at 360 nm are very small.

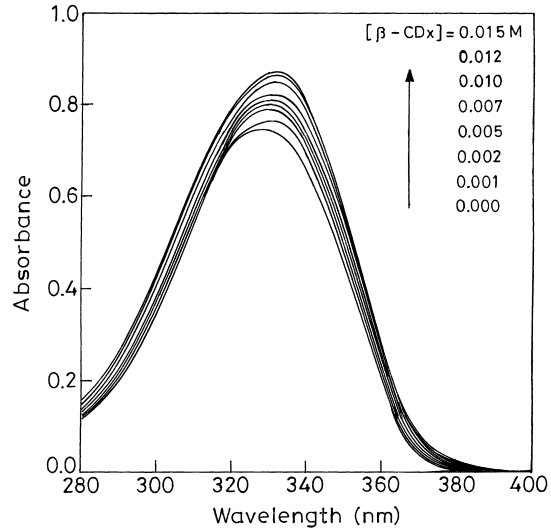

Fig. 1. Absorption spectrum of DMAPBI at different β-CDx concentrations. [DMAPBI] = 2×10^{-5} M, pH = 8.0.

Further, no change is observed in the absorbances of the solutions when recorded after 4–5 h.

Fig. 2 represents the fluorescence spectrum of DMAPBI in different amounts of β-CDx at pH 8. Since no clear isosbestic point was observed in the absorption spectrum of neutral DMAPBI, the excitation wavelength (360 nm) is selected in such a manner that the absorbance changes are minimum. Both the emission bands (A and B) are blue shifted. The blue shift observed in the A band (10 nm) is larger than that observed in the B band (6 nm). The increases

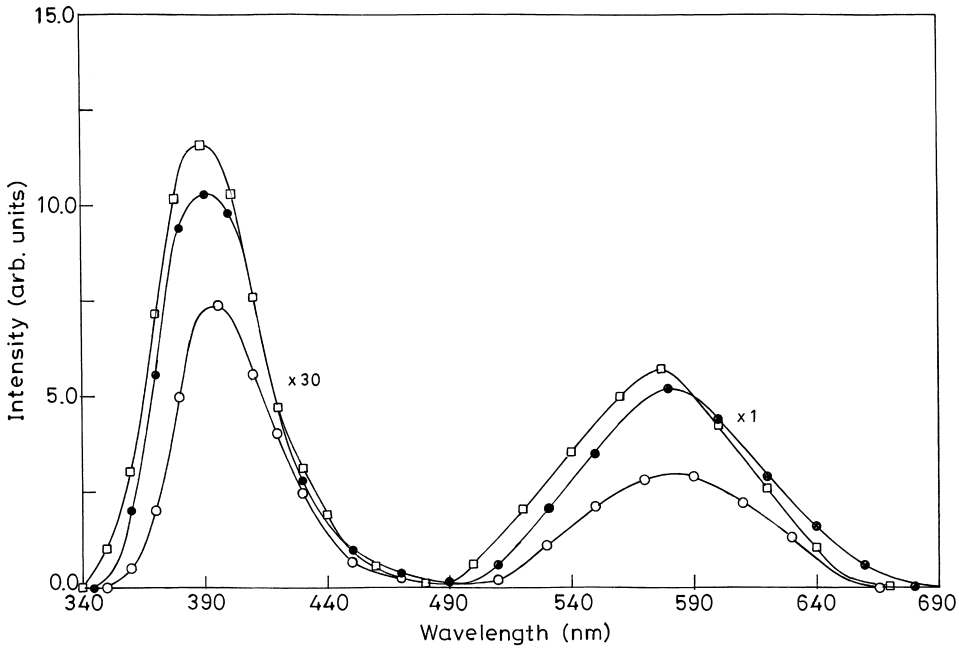

Fig. 2. Fluorescence spectra of DMAPBI at different concentrations of β-CDx: 0.0 M (o–o–o), 0.005 M (•–•–•), 0.010 M (———). [DMAPBI] = 2×10^{-5} M, λ_{exc} = 360 nm, pH = 8.0.

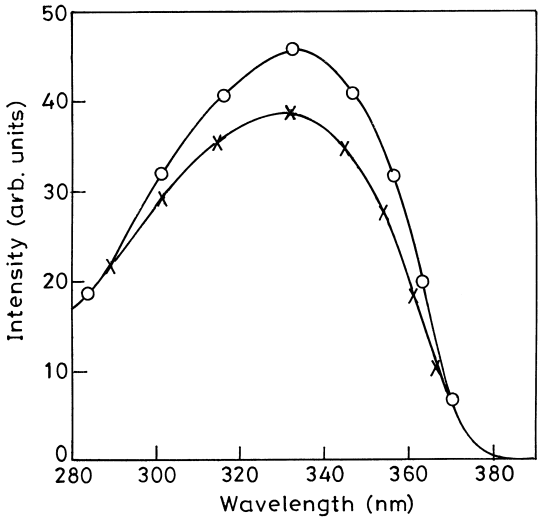

Fig. 3. Fluorescence excitation spectra of DMAPBI recorded at 390 nm (○–○–○) and 590 nm (x–x–x). [DMAPBI] = 2×10^{-5} M, pH = 8.0.

in ϕ_{fl}^{A} and ϕ_{fl}^{B} is 1.9 and 1.6 times, respectively, when compared with those in aqueous medium. Increase in the fluorescence intensities of both the bands level off at ~0.01 M β-CDx. These changes can also be seen as the formation of the inclusion complex of DMAPBI with β-CDx.

Fluorescence characteristics of both the bands of neutral DMAPBI were also studied by using different λ_{exc} and it was found that both band maxima and ϕ_{fl} of both bands were independent of λ_{exc}. This suggests that the emissions occur from the completely relaxed states and that the relaxation times of the environments around DMAPBI are much smaller than the radiative lifetime. Fluorescence excitation spectra (Fig. 3) recorded at $\lambda_{em} = 390$ and 590 nm emissions are exactly similar to each other as well as to the absorption spectrum. This suggests that the ground state precursor is the same for both bands, as observed in aqueous medium.

Fluorescence decay observed in both emissions followed a single exponential and lifetimes calculated for both bands were found to be equal (1.20 ns). These values are greater than those observed in water (0.8 ns). This indicates that, as in aqueous medium, the equilibrium between the B state and the A state is also observed in β-CDx in a short time. The values of the radiative (k_r) and non-radiative (k_{nr}) decay rate constants were calculated using the relations

$$k_r = \left(\frac{\phi_{fl}}{\tau}\right), \qquad k_{nr} = \left(\frac{1}{\tau}\right) - k_r$$

The values of k_{nr} for the normal emission in water and 0.01 M β-CDx were found to be 3.34×10^8 and 8.3×10^6 s^{-1}, respectively. The similar values for the A band could not be calculated due to the non-availability of accurate and absolute ϕ_{fl}^{A}, as mentioned earlier [27], but the increase in ϕ_{fl}^{A} and τ_A in β-CDx suggests that the value of k_{nr} for the A band will decrease when solubilized in β-CDx.

As mentioned earlier, no isosbestic point is observed in the absorption spectrum and thus one can rule out the possibility of the formation of a well defined 1 : 1 complex. But based on the results of *p*-(*N*,*N*-dimethylamino)- [28] and *p*-(*N*,*N*-diethylamino)benzoic acid [17], it cannot eliminate completely the possibility that the DMAPBI/β-CDx complex is 1 : 1. Thus we have used the fluorescence data (as the variation in the fluorescence intensities is much larger than that in the absorbance) to calculate the binding constant (K_B) of DMAPBI with β-CDx using the following equation [29–31]:

$$\frac{1}{(I - I_0)} = \frac{1}{(I_1 - I_0)} + \frac{1}{\{K_B(I_1 - I_0)[\beta\text{-CDx}]\}}$$

where [β-CDx] represents the concentrations of β-CDx, and I_0 and I are the fluorescence intensities in the absence and the presence of β-CDx, respectively. I_1 is the same when DMAPBI is completely solubilized in β-CDx. A linear relation is observed when $1/(I - I_0)$ is plotted against 1/[β-CDx] (Fig. 4), thus suggesting 1 : 1 stoichiometry in the DMAPBI/β-CDx complex. The values of K_B obtained from the slopes using different analytical wavelengths agree within the error limit of 485 ± 10 M^{-1}. Even larger values for K_B have been observed [12] for similar molecules forming the 1 : 1 inclusion complex.

The spectral characteristics of DMAPBI have been studied very well [27]. The LW absorption band maximum is red shifted with an increase in the polarity of the solvents only, whereas it is slightly blue shifted with an increase in the protic nature of the solvents. Dual fluorescence (A and B) is observed in all the solvents and the fluorescence band maximum of the A band is more sensitive than that of the B band. ϕ_{fl}^{B} is nearly unity in all the solvents except water (0.73), whereas the fluorescence intensity of the A band increases up to the polar/aprotic solvents and then decreases with an increase in the protic nature of the solvents. This has been attributed to the greater stabilization of the highly polar TICT state by strong dipole–dipole and hydrogen bond interaction with protic solvents, and consequently, rapid non-radiative transition to the ground and/or low lying triplet state [13,14]. Fluorescence excitation spectra recorded at both bands resemble each other and the absorption spectrum, hinting at the same ground state precursor for both emissions.

Based on the above results and considering our results in the present study, it may be concluded that the 1 : 1 inclusion complex is formed between DMAPBI and β-CDx at pH 8, as shown in Scheme 1. This is based on the following observations: the ground state geometry of DMAPBI was optimized using the AM1 method [29] (QCMP 137, MOPAC6/PC), the vertical distance between H_{30} and H_{33} is 5.11 Å, the horizontal distances between H_{31} and H_{20}, H_{32} and N_3, and H_{22} and N_3 are 11.58, 4.66 and 6.92 Å, respectively. Considering the shape and the dimensions of DMAPBI and β-CDx [30,31], DMAPBI can enter β-CDx lengthwise in two ways, as shown in Scheme 1 (a–b). If the inclusion complex is

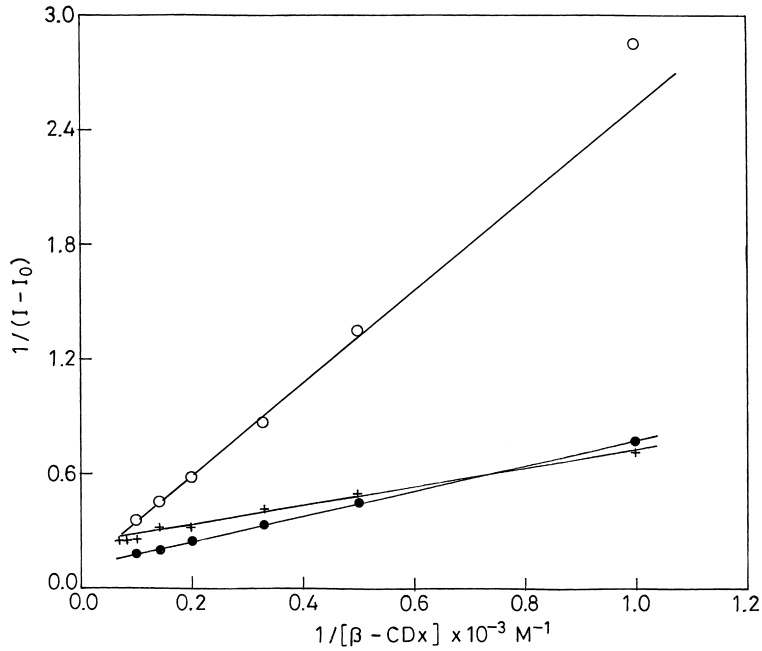

Fig. 4. Plot of $1/(I - I_0)$ versus 1/[β-CDx] at pH 8.0 (+–+–+) and at pH 4.0 at 400 nm (○–○–○), 520 nm (•–•–•).

formed as shown in Scheme 1 (a), the –NMe_2 group will be present in the bulk water phase and thus will experience the same kind of solvation at –NMe_2 as experienced in aqueous medium. Thus no change would be observed in the absorption and the fluorescence band maxima, especially of A band, as well as in its ϕ_{fl}^{A}. On the other hand, if DMAPBI is present as shown in Scheme 1 (b): (i) the –NMe_2 group would be buried in the hydrophobic cavity and then the bulk water would not be available to solvate it. This would eliminate the solvation shell around the –NMe_2 group, and thereby, blue shifts in both bands, and (ii) =N– atom will be present near the interface of the bulk water phase and the rim of β-CDx. This will lead to a pK_a value of the protonation reaction of =N– atom, similar to that observed in aqueous medium. Observation of nearly similar pK_a and spectral characteristics of the monocations of DMAPBI in β-CDx confirm the inclusion of DMAPBI in β-CDx (see later) as shown in Scheme 1 (b). The presence of only one kind of inclusion complex is further substantiated (i) by the resemblance between the excitation spectra recorded in water and those recorded in aqueous β-CDx, and monitored at SW and LW emissions, (ii) by there being only one lifetime when monitored at 400 and 580 nm, (iii) by the large value of K_B, the large value of the association constant implying that DMAPBI is tightly embedded in the β-CDx cavity and (iv) from the results of Kim et al. [17] that have shown the presence of *N*,*N*-diethylamino group (which is larger than –NMe_2) in *p*-(*N*,*N*-diethylamino)benzoic acid in the β-CDx cavity.

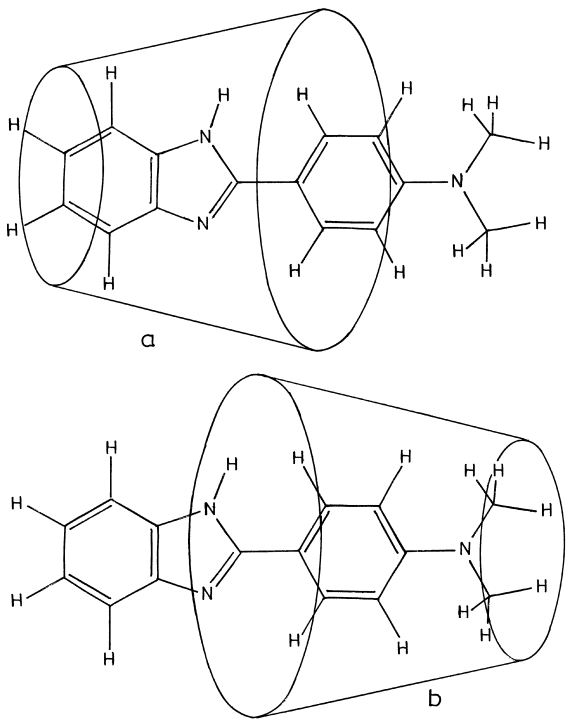

Scheme 1.

The kinetics of the TICT process has been explained by the mechanism proposed by Kajimoto et al. [32]:

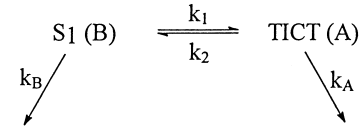

where k_1 and k_2 depict the fast decay of the B and A bands, respectively, that is complete within few picoseconds. k_B and

k_A depict the sum of the radiative and non-radiative decay rates. On account of the limitation of our time resolved instrument, we are unable to observe these decays. Since the decay time of the slow component of the B emission is similar to that of the A emission within the experimental error, it may be concluded that the equilibrium between the B state and the A state is also achieved in β-CDx in a rather short period. This behaviour is similar to that observed in aqueous medium.

It is now well established that the energy barrier for the TICT process decreases with the increase in the polarity of the solvents [33,34]. This means that the fluorescence intensity of the B band will increase and that of the A band will decrease if the polarity of the environment decreases. The blue shifts observed in both bands (A and B) clearly establish that the β-CDx cavity is less polar than the aqueous phase. The enhancement in the fluorescence intensity of the B band can be explained on the above-given lines, whereas the opposite results observed for the A band can be explained as follows. In the less polar environment of β-CDx, the dipole–dipole interactions between the environment in β-CDx and the A state will be lowered. Due to this, the energy gap between the A state and the Franck–Condon ground state will increase, and this is supported by the blue shift observed in the A emission. The increase in the energy gap reduces the rate of non-radiative transition from the A state and thus enhances the A emission. Although we have not been able to measure the values of k_{nr} for the A state, the increase in the value of τ_A and the relative increase in the fluorescence intensity qualitatively support the decrease in the value of k_{nr} for the A emission. The decrease in the value of k_{nr} for the B band on going from water to β-CDx environment also supports the enhancement in the B emission.

Based on the results of Kim et al. [17], (i.e. *–N,N*-diethylamino group is present in the cavity), the large increase in the fluorescence intensity of the A band in β-CDx suggests that the free rotation of the $–NMe_2$ group is still possible in the β-CDx cavity. Considering that the TICT emission was observed in solid matrices and/or under high pressure [35], it can be concluded that the restriction on the increased viscosity in the β-CDx cavity does not forbid the formation of the A state. It may also be mentioned that the TICT phenomenon for DMAPBI, also similar to *p*-(*N,N*-dimethylamino)benzonitrile [33–35], is more dependent on the polarity of the medium rather than on free rotational motion (e.g. viscosity).

3.2. Prototropic species in aqueous medium

Fig. 5 depicts the absorption spectrum of DMAPBI in aqueous medium at different acid concentrations in the range of pH 4 to 8. The results observed agree with the earlier observations [27], i.e. the same band maxima of the neutral (N) and the monocation (MC), only one isosbestic point at 339 nm and the same pK_a value for the MC–N equilibrium (5.6).

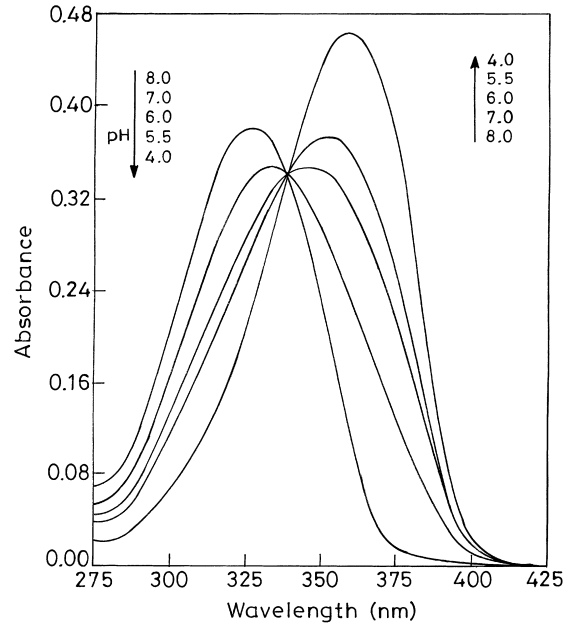

Fig. 5. Absorption spectrum of DMAPBI in aqueous medium at different acid concentrations. [DMAPBI] = 1×10^{-5} M.

Fig. 6 depicts the fluorescence spectra of the MC of DMAPBI in aqueous medium when excited at different wavelengths. At all λ_{exc}, the most intense fluorescence band is at 409 ± 5 nm, which is red shifted when compared to the B band (396 nm) and also agrees with the earlier results [27]. At $\lambda_{exc} \leq 300$ nm, a weak emission is also observed with no clear band maximum (~360 nm), but which is certainly blue shifted with respect to the B band and is absent at $\lambda_{exc} \geq 300$ nm. A slight red shift (405–414 nm) is observed in the LW emission band of the MC when λ_{exc} is increased towards red, from 280 to 380 nm. This suggests that the absorption spectrum includes the contributions from the different types of MCs or their conformers. Observation of the SW band of the MC is different from the earlier results [27] in the sense that we did not use $\lambda_{exc} < 300$ nm. The relevant data are compiled in Table 1.

Fluorescence excitation spectra have been recorded at different λ_{em}, but Fig. 7 depicts the fluorescence excitation spectra of the MC recorded at 350, 440 and 520 nm only. The results of Fig. 7 clearly indicate that there are two types of MCs in the ground state: the fluorescence excitation spectrum recorded at 350 nm is large blue shifted (302 nm) in comparison to those (360 nm) recorded at λ_{em} 440 nm. The fluorescence decays have been recorded at four emission wavelengths (380, 410, 440 and 480 nm). All these decays followed a single exponential with a lifetime of 0.25 ± 0.03 ns. The excited state lifetime of the MC could not be recorded at $\lambda_{em} < 380$ nm because of poor intensity. The relevant data are compiled in Table 2.

DMAPBI possesses two basic centres where protonation can take place. One is the $–NMe_2$ group (MC1) and the other is =N– atom (MC2). AM1 semi-empirical quantum mechan-

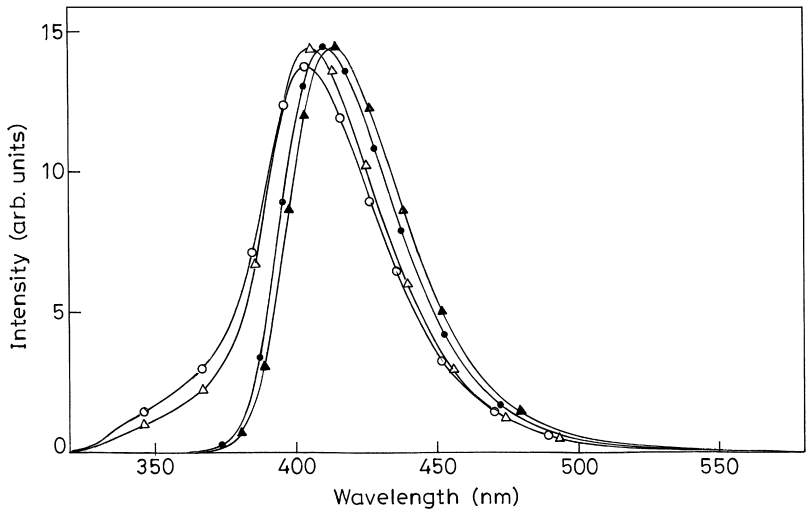

Fig. 6. Fluorescence spectrum of the MC's of DMAPBI (pH 4.0) using different λ_{exc}: 280 nm (○–○–○), 300 nm (△–△–△), 360 nm (•–•–•), 380 nm (▲–▲–▲) (for comparison, all spectra are given in the same scale).

Table 1
Absorption band maxima (λ^{ab}_{max}, nm), log ϵ_{max}, fluorescence band maxima (λ^{fl}_{max}, nm), fluorescence quantum yield of DMAPBI and its monocations in aqueous and 0.01 M β-CDx media

Medium	Neutral (pH 8.0)			Monocation (pH 4.0)		
	λ^{ab}_{max}	λ^{fl}_{max}		λ^{ab}_{max}	λ^{fl}_{max}	
		A[a]	B			
Water	328 (4.22)	586 (24)	396 (0.73)	360 (4.29)	411 (0.01)	360[b]
β-CDx	333 (4.29)	577 (45)	390 (∼1.0)	360 (4.30)	408 (0.04)	360[b]

[a] Vaules in brackets represent area under uncorrected band.
[b] $\lambda_{exc} < 300$ nm.

ical calculations [29] (QCMP 137, MOPAC6/PC) were carried out on both the MCs after optimizing their geometries in the S_0 state. Heat of formation (ΔH_f°), total energies under isolated conditions (E_{isol}) and solvated conditions (E_{sol}), the dipole moment (μ_g), the dihedral angles (θ) between the $-NMe_2$ group and the phenyl moiety and (ϕ)

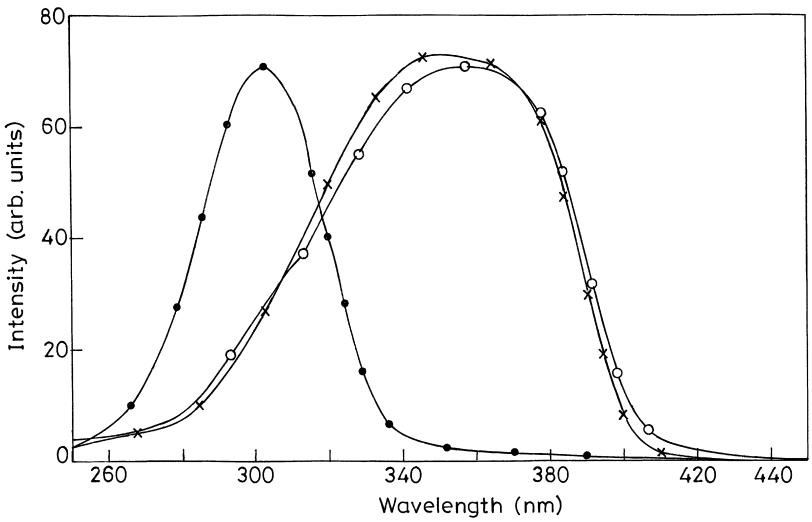

Fig. 7. Fluorescence excitation spectrum of the MC's of DMAPBI (pH 4.0) using λ_{em}: 350 nm (•–•–•), 440 nm (x–x–x), 520 nm (○–○–○) (for comparison, all spectra are given in the same scale).

Table 2
Lifetimes (ns) of the neutral and the monocation of DMAPBI in aqueous and 0.01 M β-CDx media

Species	λ_{exc}	λ_{em}	Water	β-CDx			
	(nm)	(nm)	τ_1	τ_1	A_1	τ_2	A_2
Neutral (pH 8.0)	332	390	0.80(τ_B)	1.20(τ_B)	–	–	–
	–	580	0.85(τ_A)	1.20(τ_A)	–	–	–
Monocation (pH 4.0)	354	380	0.27	0.51	–	–	–
	–	410	0.26	0.48	–	–	–
	–	440	0.26	0.46	–	–	–
	–	480	0.21	0.50	55.1	34.3	44.9
	–	500	–	0.50	34.8	35.5	65.2

between the benzimidazolyl moiety and phenyl ring are compiled in the Scheme 2. The dipolar solvation energies (in water) were calculated by using the equation [36,37]

$$E_{sol} = E_{isol} - \left(\frac{\mu^2}{4\pi\epsilon_0 a^3}\right) f(\epsilon)$$

where $f(\epsilon) = (\epsilon - 1)/(2\epsilon + 1)$. μ is the dipole moment, a is the Onsager cavity radius and ϵ is the static dielectric constant.

It is well established [38] that if $\pi \rightarrow \pi^*$ is the first excited singlet state transition, the protonation at the amino group leads to the blue shift, and that at =N– atom leads to the red shift in the absorption and fluorescence spectra of the neutral molecules. Based on the fluorescence excitation spectra and the fluorescence spectra, 302 nm in the fluorescence excitation spectra and 360 nm in the fluorescence emission spectra can be assigned to the MC1, whereas 360 nm in the fluorescence excitation spectra and ~410 nm in the emission spectra can be assigned to the MC2. These assignments are consistent with the results obtained by AM1 calculations (Scheme 2). For example, dihedral angles ϕ (between the two rings) are nearly similar in the neutral and both the MCs, but the dihedral angles (θ, between the amino group and the phenyl ring) are 16°, −117° and −0.5° for the neutral, the MC1 and the MC2, respectively. Due to the planarity of the –NMe_2 group in the MC2, the conjugation between the two rings and the resonance interaction of the –NMe_2 group with the heterocyclic ring will increase. This will lead to the structure MC'2:

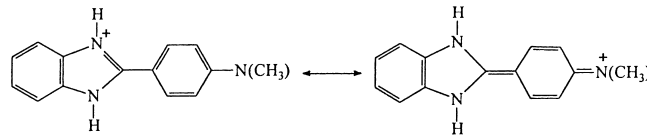

which further stabilizes the MC2 and thus leads to a large red shift in the absorption spectrum of the MC2. Since the lone pair of electrons on the amino group in the MC1 are not free to participate in the delocalisation with the π-cloud, a blue shift would occur. The agreement between the band maximum (299 nm) of 2-phenylbenzimidazole (2-PBI) [39] and that of the MC1 further substantiates the above-given explanation.

Unlike the MC1 of 2-(4′-dimethylaminophenyl)benzothiazole (DMAPBT) (where the absorbance at 302 nm and the fluorescence intensity at 390 nm when excited at 302 nm were quite large) [27], no clear absorption band maximum at 302 nm and weak fluorescence intensity of the MC1 of DMAPBI can be explained as follows. Firstly, the pK_a value for the protonation of =N– in 2-phenylbenzimidazole is 5.3 [39], whereas in 2-phenylbenzothiazole, it is 0.7 [40]. It is already clear from the data in Scheme 2 that the –NMe_2 group in the MC2 is nearly coplanar (−0.5°) with the aromatic ring in the S_0 state. Consequently, the lone pair orbital of –NMe_2 overlaps with the π-cloud of the aromatic ring. This decreases the charge density at the –NMe_2 group, but increases the same on =N– atom, thereby increasing the probability for the first protonation at =N– atom by increasing the pK_a value to 5.6 and decreasing the pK_a (~4.5) [38] of the –NMe_2 group. In other words, the amount of the MC1 at such an acid strength will be quite small. On the other

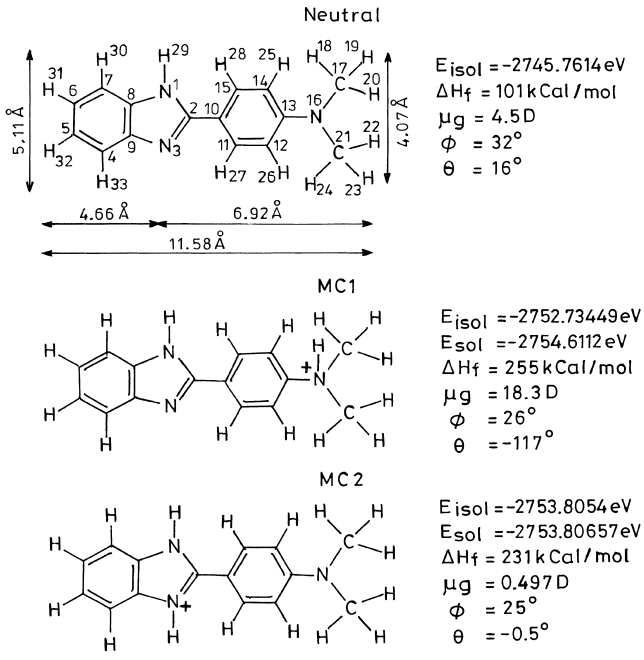

Scheme 2.

hand, based on the total energy (Scheme 2), it is clear that the MC2 is more stable in isolated condition, by 155 kJ mol^{-1}, than the MC1, but in aqueous medium, adding the solvation energies, the MC1 becomes more stable than the MC2 by 54.8 kJ mol^{-1}. This is so because the dipole moment (μ_g) of the MC1 (18.3 D) is very large in comparison to that of the MC2 (0.5 D). This argument can be rejected on the ground that the AM1 model only considers the final stage of the MC and does not take into account the acid strength of aqueous medium. Secondly, we have also calculated the global minima at the basic centres using the potential energy mapping programme [41]. This method considers the charge density at a particular basic centre of interest plus the effect of charges of the rest of the atoms in the molecules. The greater the depth of the potential well, the greater are the chances of protonation at the basic centre. Fig. 8 represents the electrostatic potential energy map for DMAPBI. The result clearly shows that the =N– site is more reactive than –NMe_2 as the minima of the potential well at =N– is −122.3 kJ mol^{-1}, whereas at –NMe_2, it is only −61.2 kJ mol^{-1}.

The small red shifts observed with the increase in λ_{exc} could be due to the presence of different resonating structures as shown above and thus there may be little difference in their solvation energies. The broadness in the excitation spectra recorded at 440 and 520 nm (Fig. 7) could be due to the presence of such resonating structures which are in equilibrium with each other. This is confirmed by the presence of single exponential decay in the fluorescence intensity and the possession of a similar lifetime when monitored in the wavelength region 380–480 nm.

3.3. Effect of β-CDx on the prototropic reaction of DMAPBI

The absorption spectrum of DMAPBI has been studied in 0.01 M β-CDx aqueous solution in the pH range 4–8. The isosbestic point observed at 342 nm hints at the equilibrium between the MC–N species. No change is observed in the absorption band maximum (360 nm) of the MC of DMAPBI in β-CDx when compared with that in aqueous medium. Similarly, the pK_a value for the MC–N equilibrium of DMAPBI in 0.01 M β-CDx and in aqueous medium, determined using absorption data, are found to be 5.8 and 5.6, respectively. Fig. 9 depicts the effect of β-CDx concentration of the MC (pH 4) of DMAPBI. As in the case of the absorption spectrum of the neutral DMAPBI, no clear isosbestic point is observed in the absorption spectrum of the MC of DMAPBI when β-CDx concentration is varied. But at the same time, hardly any change is observed in the absorbance at the band maximum (360 nm) or towards the red or blue side of the band maximum.

Fig. 10 depicts the fluorescence spectrum of the MC of DMAPBI in 0.01 M β-CDx using different λ_{exc}. As in the case of aqueous medium, the SW emission band (360 nm) along with the LW (∼410 nm) emission band is only observed when $\lambda_{exc} < 300$ nm. The LW emission band of the MC in aqueous medium and in β-CDx are similar to each other for λ_{exc} 280 and 300 nm, whereas it is blue shifted by 3–5 nm for λ_{exc} 360 and 380 nm in β-CDx when compared with those in aqueous medium. Unlike in the case of aqueous medium, the fluorescence band maximum of the MC in β-CDx environments does not vary much with the change in λ_{exc}. The emission intensities of 360 and 410 nm bands

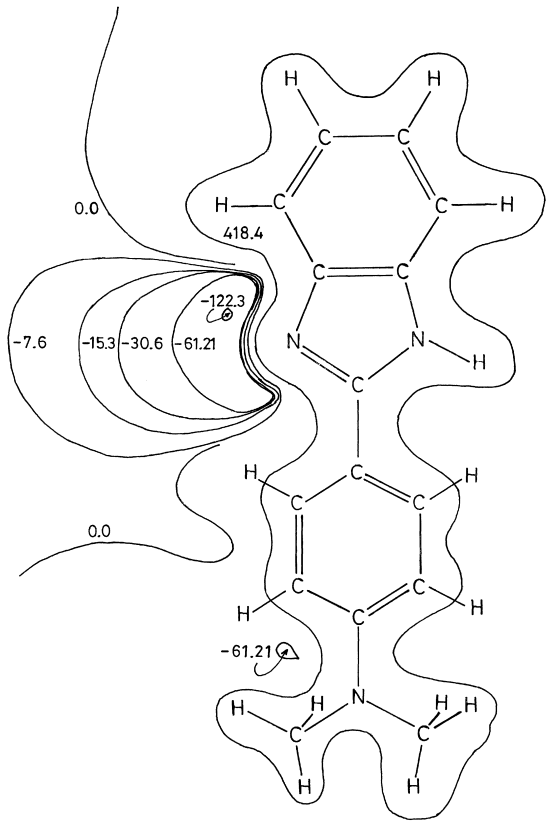

Fig. 8. Electrostatic potential map for DMAPBI in the ground state (values shown are in kJ mol^{-1}).

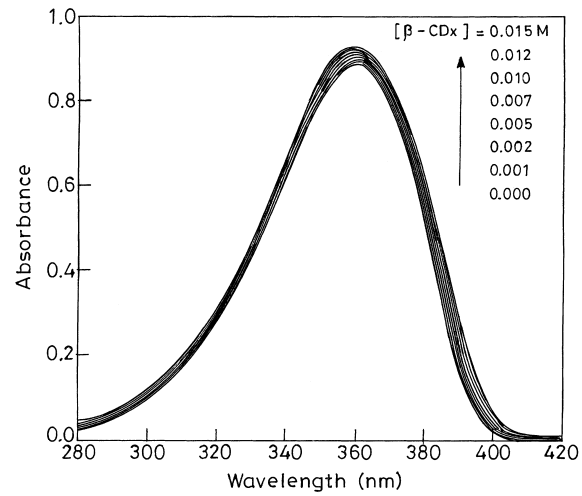

Fig. 9. Absorption spectrum of the MC's of DMAPBI (pH 4.0) at different concentrations of β-CDx. [DMAPBI] = 2×10^{-5} M.

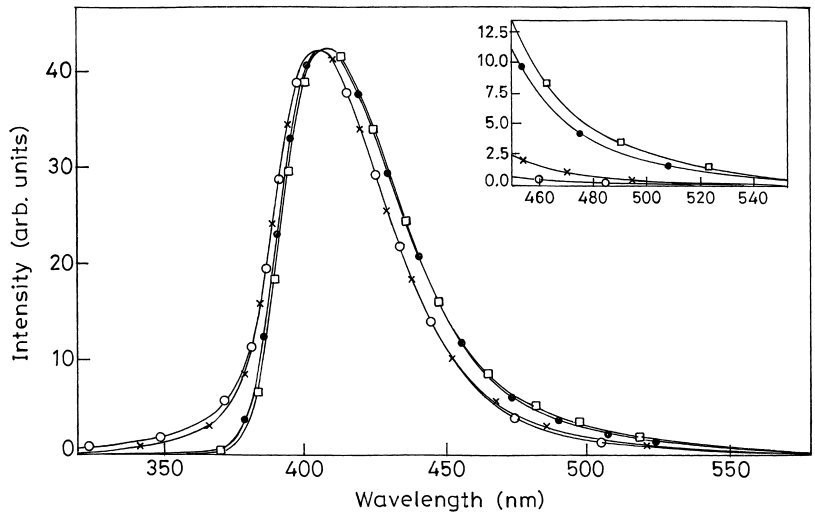

Fig. 10. Fluorescence spectrum of the MC's of DMAPBI (pH 4.0) in 0.01 M β-CDx when excited at different λ_{exc}: 280 nm (○–○–○), 300 nm (x–x–x), 360 nm (•–•–•), 380 nm (———). [DMAPBI] = 2×10^{-5} M (for comparison, all spectra are given in the same scale). The inset box shows the fluorescence spectrum of the MC of DMAPBI (450–550 nm) in the expanded scale.

decreased and increased by a factor of 42% and 43%, respectively, when compared to those in water. Besides these changes, the intensity of the red part of the 410 nm emission band is more intense in β-CDx than those in aqueous medium (see the inset box in Fig. 10).

The fluorescence excitation spectra of the MC of DMAPBI in 0.01 M β-CDx were recorded at 350, 440 and 520 nm (Fig. 11). The results observed at λ_{em} 350 nm (λ_{max}^{exc} 308 nm) and at λ_{em} 440 nm (λ_{max}^{exc} ~360 nm) are similar to those observed in aqueous medium, but using λ_{em} 520 nm, besides the main peak at ~360 nm, a shoulder appears at ~380 nm, which is different from that observed in aqueous medium. This hints at the presence of another ionic species which is different from that having the emission maximum at ~410 nm or the formation of some inclusion complex between the MC and β-CDx.

The fluorescence decay of the MC of DMAPBI in 0.01 M β-CDx was measured by excitation at 332 and 354 nm and monitoring at five different wavelengths. The relevant data are compiled in Table 2. It is evident from the data in Table 2 that a single exponential decay is observed at λ_{em} 380, 410 and 440 nm, whereas the emission at 480 and 500 nm follows double exponential. The lifetime of the short-lived species in the double exponential is similar to that obtained from the single exponential analysis, except that the relative amplitude of the short-lived species keeps on decreasing as λ_{em} increases. Further, emission decay analysis carried out at longer channels followed single exponential with lifetime, agreeing with the lifetime of the long-lived ionic species in the double exponential. It is further noticed that the lifetimes of the ionic species in β-CDx are longer than those observed in aqueous medium and

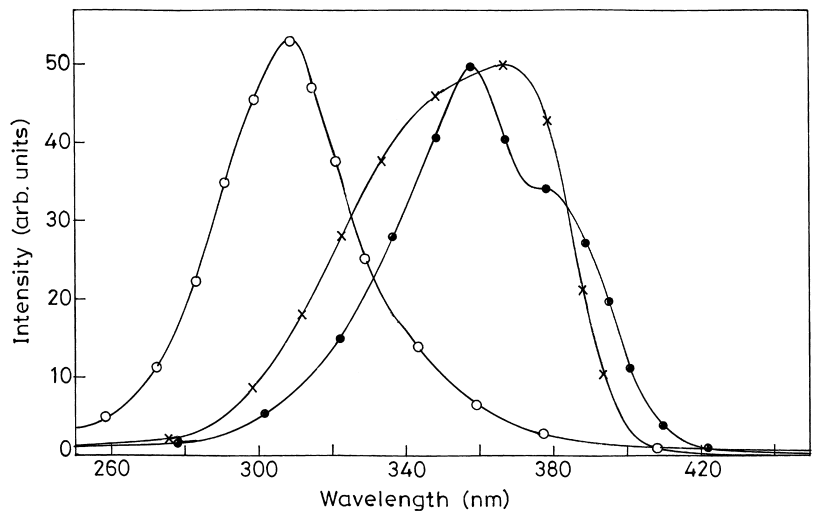

Fig. 11. Fluorescence excitation spectrum of the MC's of DMAPBI (pH 4.0) in 0.01 M β-CDx monitored at different emission wavelengths: 350 nm (○–○–○), 440 nm (x–x–x), 520 nm (•–•–•). [DMAPBI] = 2×10^{-5} M (for comparison, all spectra are given in the same scale).

are also independent of λ_{exc}. As in the case of the fluorescence excitation spectra, the lifetime data also support the presence of two kinds of inclusion complexes.

Based on the same arguments as given for the neutral species of DMAPBI, we have used the fluorescence data (Fig. 4, λ_{exc} 360 nm) to calculate the binding constants of the MC of DMAPBI using the same equation and different analytical wavelengths. Unlike the results of the neutral species, the K_B for the MC obtained using analytical wavelengths 400 and 420 nm is $180 \pm 5\ M^{-1}$, whereas the values of K_B obtained for wavelengths 500 and 520 nm measure only $42 \pm 7\ M^{-1}$. The error in the latter value of K_B is large because of the smaller fluorescence intensity. Similar values of K_B (within error limits) obtained using 500 and 520 nm as analytical wavelengths show that the contribution of the 410 nm emission to the 500 nm emission band is negligible.

Spectral characteristics, the values of the binding constants and the pK_a value of the MC–N equilibrium support our earlier conclusion arrived in Section 3.1 that DMAPBI forms the inclusion complex with β-CDx as shown in Scheme 1 (b). This is based on the following arguments:

1. =N– atom of DMAPBI, as shown in the inclusion complex in Scheme 1 (b), lies near the interface of the β-CDx rim and bulk aqueous phase. Thus the spectral characteristics of the MC are nearly similar to those observed in aqueous phase. Similar results are also observed when prototropic equilibrium also occurs at the interface of the micellar system [42–44].
2. The fluorescence intensity of the MC1 (360 nm) decreases and that of the MC2 (410 nm) increases with the increase in β-CDx concentration. It is well known that the pK_a value for the protonation reaction decreases with the decrease in the polarity or because they are unstable [45]. Thus, the protonation of the MC1 will decrease in the inclusion complex shown in Scheme 1 (b). Further, not only is it well known that the $-NH_3^+$ ion is a strong acid in the S_1 state [46] in aqueous medium, but it is also well established that the acid strength of the $-NH_3^+$ ion decreases as the polarity decreases [47,48]. Our results are opposite to this observation. The increase in the fluorescence intensity of the MC2 could be due to the decrease in the non-radiative process in β-CDx ($k_{nr} = 3.8 \times 10^9$ and $1.75 \times 10^9\ s^{-1}$ in aqueous and β-CDx media, respectively).
3. The length of the β-CDx cavity is ~7.8 Å. If DMAPBI is located as shown in Scheme 1 (a), =N– atom (distance between H_{32} and N_3 is ~4.7 Å) will be present inside the non-polar cavity and one should observe a decrease in the pK_a for the protonation reaction of this atom, as observed in case of 2-(2′-hydroxyphenyl)benzimidazole [11]. It has also been shown by Kim et al. [17] that the pK_a values for the deprotonation of the carboxylic acid group increases to 7 in α-CDx, whereas it remains unchanged in β-CDx. They showed that the –COOH group is buried in the cavity of α-CDx, but is exposed to the aqueous phase in β-CDx. Similarly, in our study on 2-(4′-*N*,*N*-dimethylaminophenyl)-1H-napth[2,3-d]imidazole (DMAPNI) [49], the protonation constant of =N– atom in β-CDx is 5.05 in comparison to 5.65 in aqueous medium. DMAPNI forms 1 : 2 complex with β-CDx and thus =N– atom is located in the cavity of β-CDx. Our results are opposite to these observations, but similar to those of Kim et al. [17].

Lastly, fluorescence spectra, fluorescence excitation spectra, lifetime data and the values of binding constants have clearly established the presence of two kinds of 1 : 1 inclusion complexes of the MC of DMAPBI with β-CDx. The 410 nm emission band can be assigned to the MC2 as the fluorescence excitation spectrum resembles the absorption spectrum (360 nm). But we have been unable to assign the red tail, the long-lived emission and the smaller binding constant (42) of the MC to any kind of inclusion complex. One thing which is certain is that the latter inclusion complex cannot be due to the TICT state of neutral DMAPBI even if we assume (although not possible) that $-NHMe_2^+$ decomposes in the S_1 state to give the neutral species because the value of K_B for neutral DMAPBI is 482 (evaluated using the TICT analytical wavelength).

4. Conclusions

The above-given results have indicated that: (i) neutral DMAPBI and its monocation form 1 : 1 complex with β-CDx, (ii) the interior of β-CDx is less polar than the bulk aqueous phase, as established by the spectral shifts, (iii) the $-NMe_2$ group is buried in the interior of the β-CDx cavity, as shown by the spectral data and the pK_a value for the MC–N equilibrium, (iv) enhancement in the A band intensity is due to the less dipole–dipole interaction of the highly polar TICT state in the cavity of β-CDx and that the free rotation of the $-NMe_2$ group is feasible in the β-CDx cavity, and (v) the proportion of the MC1 is much smaller than that of the MC2 in aqueous medium and that it further decreases in β-CDx medium.

Acknowledgements

We are thankful to the Department of Science and Technology, New Delhi for the financial support to the Project No. SP/SI/H-39/96.

References

[1] W. Saenger, Angew. Chem. Int. Ed. Eng. 19 (1980) 346.
[2] G. Wenz, Angew. Chem. Int. Ed. Eng. 33 (1994) 803.
[3] V.K. Smith, T.T. Ndou, I.M. Warner, J. Phys. Chem. 98 (1994) 8627.
[4] G.C. Catena, F.V. Bright, Anal. Chem. 61 (1989) 905.

[5] A. Pena de la Munoz, T.T. Ndou, I.M. Warner, in: I.M. Warner, L.B. McGowen (Eds.), Spectroscopic Studies in Organized Media: An Overview, Advances in Multidimensional Luminescence, vol. 2, JAI Press, Greenwich, CT, USA, 1993, pp. 1–18.
[6] L.A. Blyshak, T.M. Rossi, G. Pantony, I.M. Warner, Anal. Chem. 60 (1988) 2127.
[7] R.A. Femia, L.J. Cline Love, J. Phys. Chem. 89 (1985) 1897.
[8] I.M. Warner, J.M. Schuette, in: I.M. Warner, L.B. McGowen (Eds.), Spectroscopic Studies in Organized Media: An Overview, Advances in Multidimensional Luminescence, vol. 2, JAI Press, Greenwich, CT, USA, 1993, pp. 61–80.
[9] J.E. Hansen, E. Pines, G.R. Flemming, J. Phys. Chem. 96 (1992) 6904.
[10] S. Santra, S.K. Dogra, J. Photochem. Photobiol. A: Chem. 101 (1996) 221.
[11] E.L. Roberts, J.K. Dey, I.M. Warner, J. Phys. Chem. 100 (1996) 19681.
[12] E.L. Roberts, J.K. Dey, I.M. Warner, J. Phys. Chem. 101 (1997) 5296 and references listed there in.
[13] A. Nag, K. Bhattacharyya, Chem. Phys. Lett. 151 (1988) 4747.
[14] A. Nag, R. Dutta, N. Chattopadhyay, K. Bhattacharyya, Chem. Phys. Lett. 157 (1989) 83.
[15] K.A. Al-Hassan, V.K.A. Klein, A. Suwaiyan, Chem. Phys. Lett. 212 (1993) 581.
[16] S. Kundu, N. Chattopadhyay, J. Photochem. Photobiol. A: Chem. 88 (1995) 105.
[17] Y.H. Kim, D.W. Cho, M. Yoon, D. Kim, J. Phys. Chem. 100 (1996) 15670 and references listed there in.
[18] E. Lippert, W. Luder, H. Boos, in: A. Mangini (Ed.), Advances in Molecular Spectroscopy, Pergamon Press, New York, USA, 1962, p. 443.
[19] K. Rotakeiwicz, K.H. Grellmann, Z.R. Grabowski, Chem. Phys. Lett. 19 (1973) 315.
[20] Z.R. Grabowski, K. Rotakeiwicz, A. Siemiarezuk, D.J. Cowley, W. Bauamann, Nouv. J. Chem. 3 (1979) 443.
[21] W. Rettig, Angew. Chem. Int. Ed. Eng. 25 (1986) 971.
[22] E. Lippert, W. Rettig, V. Bonacic-Koutecky, F. Heisel, J.A. Mieche, in: I. Prigogine, S. Rice (Eds.), Advances in Chemical Physics, vol. 68, Wiley-Interscience, New York, USA, 1987, p. 1.
[23] M.T. Bogret, A.J. Stull, J. Am. Chem. Soc. 47 (1925) 3078.
[24] S.K. Das, A. Bansal, S.K. Dogra, J. Bull. Chem. Soc. Jpn. 70 (1997) 307.
[25] S.K. Das, S.K. Dogra, J. Chem. Soc., Faraday Trans. I. 94 (1998) 139.
[26] P. Bortulos, S. Monti, J. Phys. Chem. 91 (1987) 5046.
[27] J.K. Dey, S.K. Dogra, J. Phys. Chem. 98 (1994) 3638.
[28] Y.B. Jiang, J. Photochem. Photobiol. A: Chem. 88 (1995) 109.
[29] M.J.S. Dewar, E.G. Zoebisch, E.F. Healy, J.J.P. Stewart, J. Am. Chem. Soc. 107 (1985) 392.
[30] J. Szejtli, in: Cyclodextrine Technology, Kluwer Academic Publishers, Dordrecht, The Netherlands, 1988, pp. 143–154.
[31] D.W. Cho, Y.H. Kim, S.G. Kang, M. Yoon, D.J. Kim, J. Chem. Soc., Faraday Trans. 92 (1996) 29.
[32] O. Kajimoto, T. Nayuki, T. Kobayashi, Chem. Phys. Lett. 209 (1993) 357.
[33] J.M. Hicks, M.T. Vandersall, E.V. Sitzmann, K.B. Eisenthal, Chem. Phys. Lett. 135 (1987) 413.
[34] J.M. Hicks, M.T. Vandersall, Z. Babarogic, K.B. Eisenthal, Chem. Phys. Lett. 116 (1985) 18.
[35] C. Cazezau-Dubroca, A. Peirigua, S.A. Lyazidi, G. Nouchi, Ph. Cazeau, R. Lapouyada, Chem. Phys. Lett. 124 (1986) 110.
[36] N. Mataga, T. Kubala, in: Molecular Interactions and Electronic Spectra, Marcel-Dekker, New York, USA, 1970.
[37] J.F. Letard, R. Lapouyada, W. Rettig, Chem. Phys. Lett. 222 (1994) 209.
[38] J.F. Ireland, P.A.H. Waytt, Adv. Phys. Org. Chem. 12 (1974) 159.
[39] A.K. Mishra, S.K. Dogra, Spectrochim. Acta 39A (1983) 609.
[40] J.K. Dey, S.K. Dogra, Can. J. Chem. 69 (1991) 1539.
[41] P.C. Mishra, B.P. Asthana, Quantum Chemistry, QCPE, Bulletin, Programme No. QCMP039, vol. 7, 1987, p. 176.
[42] S. Nigam, S.K. Dogra, J. Photochem. Photobiol. A: Chem. 54 (1990) 219.
[43] S. Nigam, R.S. Sarpal, S.K. Dogra, J. Colloid Interface Sci. 163 (1994) 152.
[44] S. Pandey, R.S. Sarpal, S.K. Dogra, J. Colloid Interface Sci. 172 (1995) 407.
[45] R.S. Sarpal, S.K. Dogra, J. Photochem. 38 (1987) 263.
[46] H. Shizuka, Acc. Chem. Res. 18 (1985) 141.
[47] M. Swaminathan, S.K. Dogra, J. Am. Chem. Soc. 105 (1983) 6223.
[48] A.K. Mishra, S.K. Dogra, Indian J. Chem. 24A (1985) 285.
[49] S.K. Das, S.K. Dogra, unpublished results.